

Rotating solitons supported by a spiral waveguide

Milan S. Petrović,^{1,2} Aleksandra I. Strinić,^{2,3} Najdan B. Aleksić,^{2,3} and Milivoj R. Belić²

¹*Institute of Physics, P.O.Box 57, 11001 Belgrade, Serbia*

²*Texas A&M University at Qatar, P.O.Box 23874, Doha, Qatar*

³*Institute of Physics, University of Belgrade, P.O.Box 68, 11080 Belgrade, Serbia*

We investigate numerically light propagation in a single spiral waveguide formed in a nonlinear photorefractive medium for a low spatial frequency of the waveguide rotation. We present the general procedure for finding solitonic solutions in spiral waveguiding structures, as well as the variational approach to calculate soliton parameters analytically. Solitons supported by the spiral waveguide perform robust stable rotational oscillatory motion, with the period predicted by their static characteristics, without any signatures of wave radiation or soliton decay over many rotation periods and diffraction lengths.

PACS numbers: 42.65.Tg, 42.65.Jx.

I. INTRODUCTION

Nonlinear localized structures or solitons are ubiquitous in nature [1]. Two-dimensional spatial optical solitons are spatially confined light beams that propagate in nonlinear media, usually along a well-defined propagation direction and with an appropriate transverse profile. However, in general, the beam propagation need not proceed along a straight line. Rotating propagation systems provide more interesting dynamics than their straight counterparts, because the centripetal force modifies the effect of potentials present and the interaction with the medium or other beams.

Conditions under which two self-guided light beams propagating in a medium with saturating nonlinearity can spiral about each other in a double-helical orbit are described in [2]. Numerical analysis shows that the three-dimensional propagation and interaction of mutually incoherent screening spatial solitons in real (anisotropic) photorefractive crystals typically results in an initial mutual rotation of their trajectories, followed by damped oscillations and eventually the fusion of solitons [3, 4]. Further stabilisation can be achieved by introducing a composite (rotating "propeller") soliton made of a rotating dipole jointly trapped with a bell-shaped component [5]. Ringlike localized gain landscapes imprinted in focusing cubic nonlinear media support stable higher-order vortex solitons [6].

Rotating structures in optical photonic lattices are of special interest [7]. Controlled soliton rotation in the optically induced periodic (Bessel-like) ring lattices is demonstrated in [8]. Edge states in an array of evanescently coupled helical waveguides, arranged in a graphene-like honeycomb lattice, are responsible for the photonic "topological insulation", in which light propagates along the edges of a photonic structure, topologically protected from the scattering off defects [9, 10]. The modulation causing the topological protection in "photonic graphene" was achieved by making the waveguides helical; topological protection cannot be achieved for a wave packet populating a single site [10]. Furthermore,

truncated rotating square waveguide arrays support localized (corner and central) modes that can exist even in the linear case [11]. Light control in a modulated single-mode waveguide was implemented for the first time by beam-splitting and adiabatic stabilization of light in a periodically curved optical waveguide [12]. Light can be guided in the modulated waveguide because radiation losses can be successfully suppressed under properly chosen conditions.

The starting point in understanding these curious optical phenomena is the analogy between paraxial beam propagation in an optical waveguide with a bent axis and the single-electron dynamics in an atomic system [12]. This analogy originates from the formal equivalence of the scalar beam propagation equation for the waveguide in the paraxial approximation and the one-electron temporal Schrödinger equation, represented in the Kramers-Henneberger (KH) reference frame [13]. The KH transformation, originally introduced in atomic physics to investigate the interaction of a bound electron with super-high intensity and high-frequency laser fields, is a transformation to the moving coordinate frame of the entirely free charged particle interacting with the applied electromagnetic field. For a high spatial modulation frequency of the waveguide bending, the refractive index seen by the beam in the KH frame varies so fast that the beam dynamics is governed by a cycle-averaged refractive index potential. Note that if the waveguide has been bent in the (x, z) plane, the refractive index profile corresponds to a Y splitter (i.e. the curved waveguide with a short bending period is equivalent to the Y adiabatic splitter), and the suppression of radiation losses as well as the wave packet dichotomy are natural consequences of the appearance of an adiabatic splitter in the cycle-averaged limit [12].

The first experimental observation of wave packet dichotomy and adiabatic stabilization in a periodically bent optical waveguide was reported in [14]. Adiabatic stabilization can also be achieved in a three-dimensional waveguide with a helicoidal (non-planar!) axis bending, and this effect is the optical analogue of the adiabatic stabilization of a two-dimensional atom in a high-frequency high-intensity circularly polarized laser field [15]. In such

a way, the cycle-averaged effective waveguide takes an annular shape, and the launched beam adiabatically evolves into a ring form [15, 16]. On the other hand, the three-dimensional spiraling guiding structures with a shallow refractive index in the approximation of small radius of spiraling, induce a resonant effect in the form of a coupling and periodic energy exchange between optical vortices with different topological charges [17].

In this paper, we investigate numerically light propagation in the spiraling single waveguide formed in a nonlinear photorefractive medium, in the limit of a high spatial period (low spatial frequency) of the waveguide rotation and for an arbitrary helix radius. We present a general procedure for finding exact fundamental solitonic solutions in the spiraling guiding structures, based on the modified Petviashvili's iteration method. We confirm the stability of solitonic solutions by direct numerical simulation. The existence domain of rotating solitons supported by a spiral waveguide is relatively wide: below a lower power threshold they start to radiate and above an upper power threshold they escape from the waveguide. Solitons supported by the spiral waveguide perform robust and stable rotary motion over many rotation periods and diffraction lengths, without any signatures of radiation or decay. The noise, inevitable in any real physical system, causes a regular spatial oscillation of the soliton with the period well predicted by our calculus based on the static characteristics of the soliton. We also exhibit an interesting counterintuitive example of beam spiraling. Finally, we present a variational approach to these phenomena and determine soliton parameters analytically.

II. THE MODEL

We start from the well-known paraxial wave equation for the beam propagation in a nonlinear photorefractive crystal, since it provides good agreement with experimental data. We choose a photorefractive medium because there different three-dimensional waveguide structures can be fabricated easily by use of a femtosecond laser writing [18]. In the steady-state and 3D, the model equation in the dimensionless computational space (one x or y coordinate unit corresponds to $8.5 \mu\text{m}$ and the z unit corresponds to 4mm) is given by [19, 20]:

$$i \frac{\partial \Psi}{\partial z} + \Delta \Psi + \Gamma \frac{I + I_w}{1 + I + I_w} \Psi = 0, \quad (1)$$

where Ψ is the beam envelope, Δ is the transverse Laplacian, Γ is the coupling constant, $I = |\Psi|^2$ is the laser light intensity measured in units of the background intensity, and I_w is the optically-induced spiraling waveguide intensity. We assume that the refractive index change of the waveguide channel has a radially-symmetric Gaussian shape.

The optical waveguide has a helically-twisted axis with sufficiently small frequency that a guided soliton is adia-

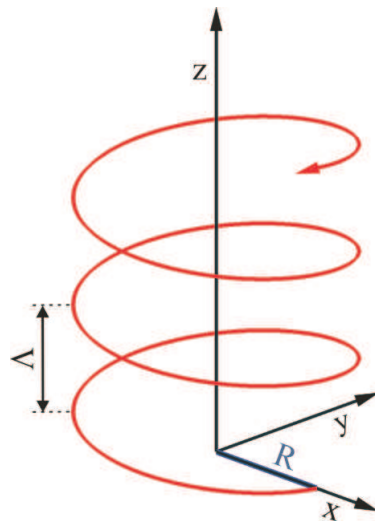


FIG. 1: Sketch of the spiral single waveguide.

batically following along the waveguide, as it rotates. We transform the coordinates into a reference frame where the waveguide is straight:

$$x' = x - R \cos(\Omega z), \quad y' = y - R \sin(\Omega z), \quad z' = z, \quad (2)$$

where R is the helix radius, Ω is the spatial frequency and $\Lambda = 2\pi/\Omega$ is the period of rotation. A single spiral waveguide is sketched in Fig. 1.

In the transformed reference frame (x', y') , the light evolution is described by:

$$i \frac{\partial \Psi}{\partial z} = \left(i \vec{\nabla}' + \frac{1}{2} \vec{N}(z') \right)^2 \Psi - \frac{1}{4} R^2 \Omega^2 \Psi + V \Psi, \quad (3)$$

where $\Psi = \Psi(x', y', z')$ is the transformed envelope, $\vec{\nabla}' = \frac{\partial}{\partial x'} \vec{e}_{x'} + \frac{\partial}{\partial y'} \vec{e}_{y'}$ the transformed gradient, $\vec{N}(z') = R\Omega[-\sin(\Omega z') \vec{e}_{x'} + \cos(\Omega z') \vec{e}_{y'}]$ the vector potential, and $V = -\Gamma(I + I_w)/(1 + I + I_w)$ the scalar potential. After the transformation $\psi(\vec{r}', z') = \Omega_T \Psi(\vec{r}', z')$ [13], where $\vec{r}' = x' \vec{e}_{x'} + y' \vec{e}_{y'}$ and $\Omega_T = \exp(\vec{\delta} \cdot \vec{\nabla}')$ is a translation operator for the vector $\vec{\delta} = -\int_0^{z'} \vec{N}(\zeta) d\zeta$, Eq. (3) is transformed in the KH reference frame and can be rewritten in the form:

$$i \frac{\partial \psi(\vec{r}', z')}{\partial z'} = -\Delta' \psi(\vec{r}', z') + V(\vec{r}' + \vec{\delta}) \psi(\vec{r}', z'). \quad (4)$$

One can see that the new wave function ψ naturally corresponds to an accelerated frame, and may be useful in different cases of noninertial frames of reference.

III. THE EIGENVALUE PROCEDURE

There are no known exact analytical solitonic solutions for our system. Owing to the symmetry and dynamics of the problem, we are searching for the self-localized wave packet continuously rotating and recreating its shape periodically (in every cycle of the rotation).

The solitonic solutions can be found from Eq. (3) by using the modified Petviashvili's iteration method [21–23]. Our system allows the existence of a fundamental soliton solution in the form:

$$\Psi(x', y', z') = a(x', y', z')e^{i\mu z'} \quad (5)$$

where μ is the propagation constant and $a(x', y', z')$ is a z -periodic complex function with period Λ . Physical requirements to obtain a rotationally-invariant solution lead to the mathematical condition:

$$\frac{\partial a}{\partial z'} = \Omega y' \frac{\partial a}{\partial x'} - \Omega x' \frac{\partial a}{\partial y'}. \quad (6)$$

After substitution of Eqs. (5) and (6) into Eq. (3), one obtains the soliton equation in a reference frame where the waveguide is straight:

$$i\Omega \left[(R \sin(\Omega z') + y') \frac{\partial}{\partial x'} + (-R \cos(\Omega z') - x') \frac{\partial}{\partial y'} \right] a$$

$$- \mu a + \Delta' a + \Gamma \frac{|a|^2 + I_w}{1 + |a|^2 + I_w} a = 0. \quad (7)$$

Next, without loss of generality, we can calculate soliton profiles at $z' = 0$. Thus, the complex-valued amplitude function $a(x', y')$, after the separation of linear and non-linear terms on different sides of the equation, satisfies a general equation

$$\mathbb{T} - i\Omega R \frac{\partial a}{\partial y'} - \mu a + \Delta' a + \mathbb{P}a = \mathbb{Q}, \quad (8)$$

where $\mathbb{T} = i\Omega(y' \frac{\partial a}{\partial x'} - x' \frac{\partial a}{\partial y'})$, $\mathbb{P} = \Gamma I_w / (1 + |a|^2 + I_w)$, and $\mathbb{Q} = -\Gamma |a|^2 a / (1 + |a|^2 + I_w)$. This equation has to be solved iteratively.

We first perform Fourier transformation of that equation, to find $\bar{a} = (-\bar{\mathbb{Q}} + \bar{\mathbb{P}}a + \bar{\mathbb{T}}) / (\mu + k_x^2 + k_y^2 + k_y \Omega R)$, where the overbar denotes the Fourier transform. Straightforward iteration of this relation unfortunately does not converge, hence we have to introduce the stabilizing factors of the form $\alpha = \int [(\mu + k_x^2 + k_y^2 + k_y \Omega R) \bar{a} - \bar{\mathbb{P}}a - \bar{\mathbb{T}}] \bar{a}^* d\mathbf{k}$ and $\beta = -\int \bar{\mathbb{Q}} \bar{a}^* d\mathbf{k}$ into the equation [23]. They do not affect the solution but improve the convergence; this procedure is the essence of the modified Petviashvili's iteration method. The following iteration equation in inverse space is obtained:

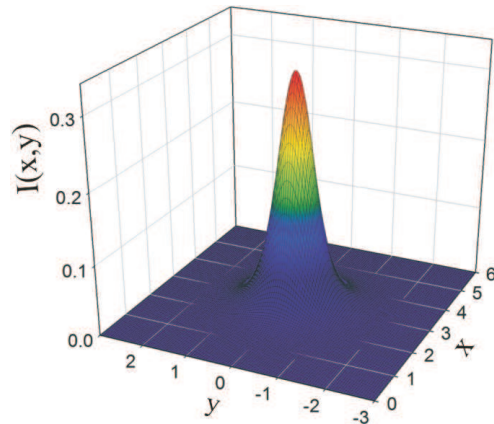


FIG. 2: Fundamental soliton intensity profile for $\mu = 2L_D^{-1}$. Parameters: $\Omega = -0.2$ rad/ L_D , $P_w = 0.044$, $R = 3$, $\Gamma = 30$.

$$\bar{a}_{m+1} = \frac{1}{\mu + k_x^2 + k_y^2}$$

$$\times \left[(\bar{\mathbb{P}}a + \bar{\mathbb{T}} - k_y \Omega R \bar{a})_m \left(\frac{\alpha}{\beta} \right)_m^{\frac{1}{2}} - \bar{\mathbb{Q}}_m \left(\frac{\alpha}{\beta} \right)_m^{\frac{3}{2}} \right], \quad (9)$$

where m counts the iterations. In this manner, stable self-consistent fundamental soliton solutions are found.

The fundamental soliton solution for $\mu = 2L_D^{-1}$ at $z = 0$ is presented in Fig. 2. We see that the optical field intensity $|a(x, y)|^2$ is almost perfectly radially-symmetric. The main quantity characterizing the spatial soliton is its power $P = \int \int I dx dy = \int \int |a(x, y)|^2 dx dy$. The imprinted spiral waveguide can be described in a similar way, because it carries its own intensity, which we take to be Gaussian: $I_w(x', y') = I_{w0} \exp[-(x'^2 + y'^2)/W_w^2]$; this gives $P_w = \int \int I_w(x', y') dx' dy' = \pi I_{w0} W_w^2$.

In this manner, one finds a family of fundamental solitonic solutions with different propagation constants and beam powers (Fig. 3) for each set of reasonable physical parameters. It is interesting to note that the existence domain is rather wide, *i.e.* although soliton widths are similar, their intensities and the corresponding potentials differ significantly from one another. The solutions are located close to the waveguide center (the helix radius $R = 3$ here) and exactly at the potential barrier minimum, as expected. Because of the saturation nature of photorefractive nonlinearity, for large intensities the potential V tends to $-\Gamma_+$ ($\Gamma = 30$ here).

The most important fundamental soliton characteristics (the soliton power, width, and peak intensity) as functions of the propagation constant are shown in Fig. 4. We see that the soliton width has a minimum value; this region corresponds to very stable rotating soliton propagation. One can notice from Fig. 4 that the obtained

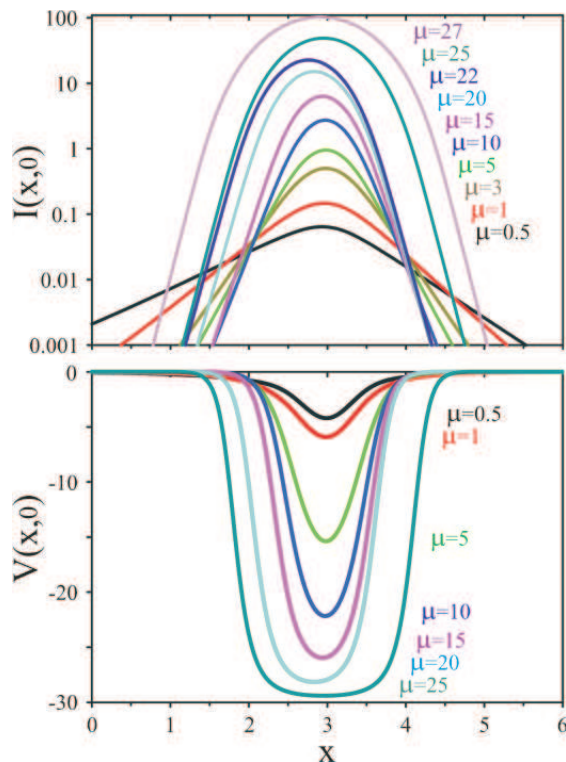


FIG. 3: Fundamental soliton intensity profiles (top) and the corresponding potential profiles (bottom) at $y = 0$. Parameters are as in Fig. 2, except $P_w=0.05$ ($I_{w0} = 0.1$, $W_w = 0.4$).

solitonic solution is stable, according to the Vakhitov-Kolokolov stability criterion [24], which claims that the solitary wave should be stable as long as $dP/d\mu > 0$. We marked the unstable solutions in Fig. 4 in red: below the lower power threshold they start to radiate, and above the upper power threshold they escape from the potential well.

IV. SOLITON DYNAMICS

In order to track the trajectory of solitons during propagation through the (nonlinear) photorefractive crystal, it is necessary to look inside the crystal volume, which experimentally is hardly feasible, because the solitons hardly radiate and are invisible from the side. Therefore, numerical simulation is preferred. Numerical procedure applied to the propagation equation is the split-step beam propagation method based on the fast Fourier transform (fourth-order symplectic algorithm). We launch a soliton (from the point $y = 0$) with an initial angular momentum in the form of an input phase tilt in the y direction, which introduces beam velocity tangential to the spiral waveguide; the helix radius is constant here, in difference to [15]. The beam can be set into a steady spiraling motion with a period dictated by the period of the helical waveguide.

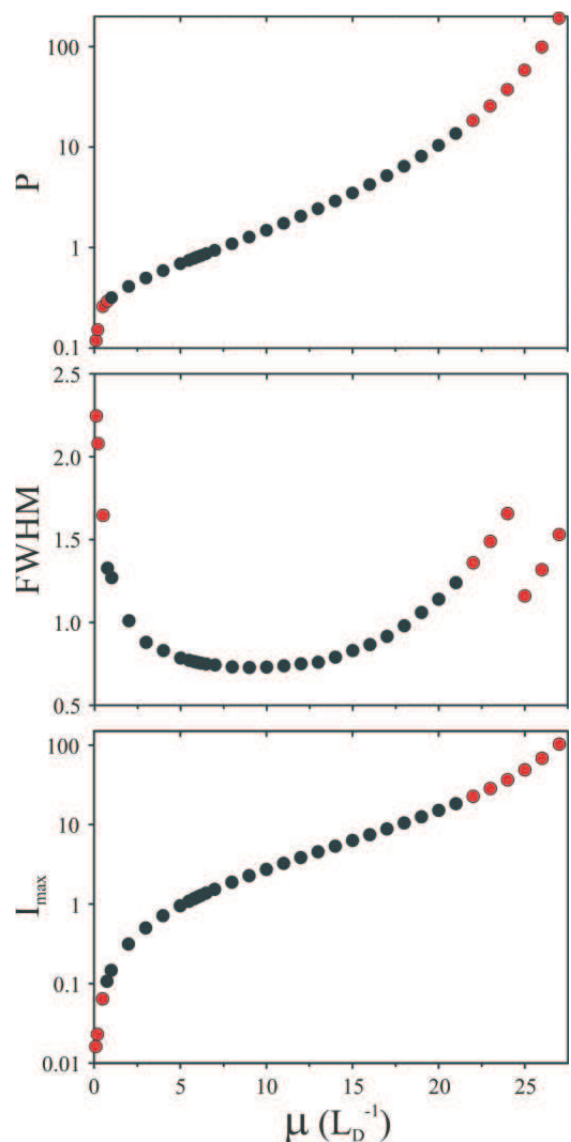


FIG. 4: Fundamental soliton power, width, and peak intensity as functions of the propagation constant. Black dots represent the stable rotary solitonic solutions, red dots the unstable solutions. Parameters are as in Fig. 3.

To check the iterative procedure for finding solitons, we propagate this input solution (in the stationary frame of reference): the peak intensity as a function of the propagation distance for several different values of the propagation constant is shown in Fig. 5. The existence domain of the rotating solitons supported by the spiral waveguide is rather wide (as presented in Fig. 4). At the lower power threshold (the case $\mu = 1L_D^{-1}$ from Fig. 5) the solitons radiate energy in the beginning. In the central part of the existence domain the fundamental solutions perform persistent stable rotary motion (the three remaining cases from Fig. 5), while the power conservation is almost perfect (although the peaks slightly oscillate). Above the upper power threshold, the solitons escape from the

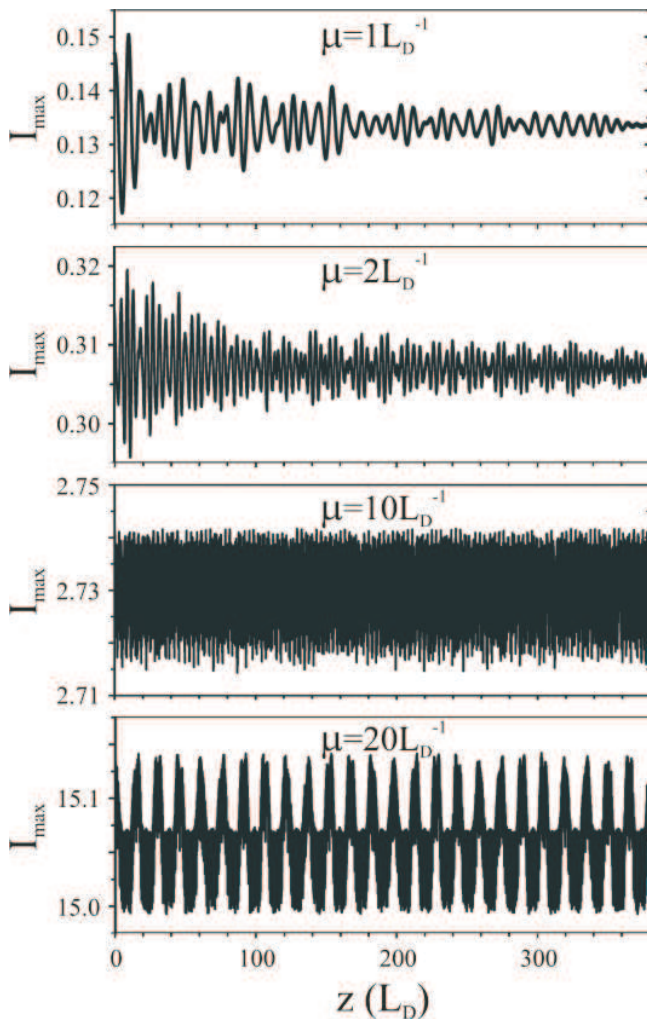


FIG. 5: Peak intensity as a function of the propagation distance for several different values of the propagation constant. Parameters are as in Fig. 3.

waveguide. On the other hand, when the rotation frequency exceeds a critical value, no localized modes can be found, since the potential barrier cannot produce the required centripetal force at such high frequencies.

The trajectory of the light beam is defined as the spatial expectation value of its transverse coordinates, weighted by the beam intensity:

$$\langle x \rangle(z) = \frac{1}{P} \int_{-\infty}^{\infty} dy \int_{-\infty}^{\infty} x |\Psi(x, y, z)|^2 dx, \quad (10)$$

$$\langle y \rangle(z) = \frac{1}{P} \int_{-\infty}^{\infty} dx \int_{-\infty}^{\infty} y |\Psi(x, y, z)|^2 dy. \quad (11)$$

A characteristic oscillatory trajectory of the rotating soliton supported by the spiral waveguide is presented in Fig. 6. Unavoidable non-ideal beam launching, which introduces numerical uncertainty in our system, causes

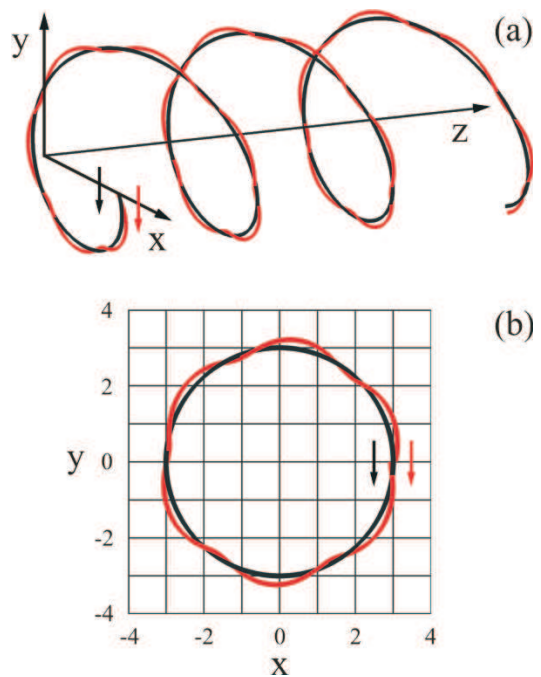


FIG. 6: Typical trajectory of a rotating soliton (red line) supported by the spiral waveguide (black line): The fundamental soliton oscillates regularly around the waveguide during propagation. (a) 3D view for the propagation distance $z = 100L_D = 3.183\Lambda$. (b) 2D view for $z = \Lambda$. Parameters are as in Fig. 3, $\mu = 15L_D^{-1}$.

a spatial oscillation of the soliton that propagates stably around the waveguide and in this way demonstrates a novel interesting type of soliton dynamics.

From Fig. 6(b), which covers one full oscillation period of the helical waveguide, one can notice that the fundamental soliton oscillates very regularly around the waveguide during propagation. We should also mention that, opposite to the breather solitons in nonlocal media where the oscillation appears in the amplitude as well as in other soliton parameters [23], here we have spatial oscillation with practically constant amplitude (see Fig. 5). Although our system is not integrable, rotating solitons supported by the spiral waveguide move self-consistently as particles in a potential created by the induced change in the refractive index [25].

An interesting question to ponder is, is it possible to connect static with dynamic characteristics of rotating solitons? The short answer is yes. Let's consider the initial soliton center position x_c , the quantity obtained in the eigenvalue procedure, shown in Fig. 7(a) as function of the propagation constant μ . We see that $x_c < R$ always; the difference is the smallest in the domain of parameter space where the solitonic solutions are stable. Because rotating solitons behave as particles, the centripetal force acting on the beam during uniform circular motion is of the form $m\Omega^2 x_c$, where m is the soliton "mass" (proportional to the soliton power P). On the other hand, there is a force associated with the potential

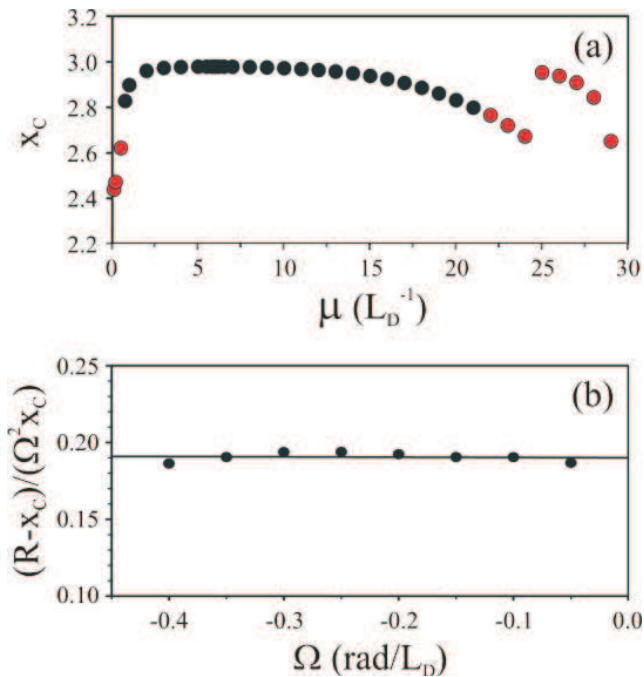


FIG. 7: (a) The initial soliton center position x_c as a function of the propagation constant μ . Black dots represent the stable rotary solitonic solutions, red dots the unstable solutions. Parameters are as in Fig. 3. (b) The quantity $(R-x_c)/(\Omega^2 x_c)$ is practically independent of the frequency of rotation Ω . Parameters are as in Fig. 3, except for $P_w=0.1$ and $P=0.5$.

created by the waveguide; in the first approximation we can consider that the force is proportional to the distance from the equilibrium (the dynamical elongation), *i.e.* of the form $k(R-x_c)$ where k is the "force constant". The two forces are equal, and if our assumption is correct, the next relation should be constant:

$$\frac{m}{k} = \frac{R-x_c}{\Omega^2 x_c} = \text{const}, \quad (12)$$

for each Ω and the constant values of both P and P_w (it is easy to understand that if $P = \text{const}$ and $P_w = \text{const}$, then also both soliton "mass" and "force constant" are constant). From Fig. 7(b) is clear that quantity $(R-x_c)/(\Omega^2 x_c)$ is independent of the frequency of rotation, and Eq. (12) is fulfilled.

Now when we know the nature of interaction in our system, we can understand dynamics of oscillating spatial solitons better. Owing to the analogy with stretched spring, harmonically oscillating solution is expected for sufficient small oscillation amplitudes, with the period

$$T = \frac{2\pi}{\Omega} \sqrt{\frac{R-x_c}{x_c}}. \quad (13)$$

The period of small oscillations T as a function of the propagation constant is represented in Fig. 8. To check

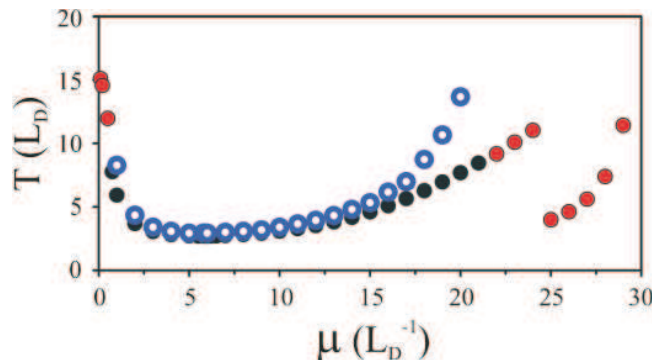


FIG. 8: The period of small oscillations T as a function of the propagation constant. For the stable (black dots) and unstable (red dots) rotating solitons period is given by Eq. (13); blue dots represent results obtained in numerical simulations. Parameters are as in Fig. 3.

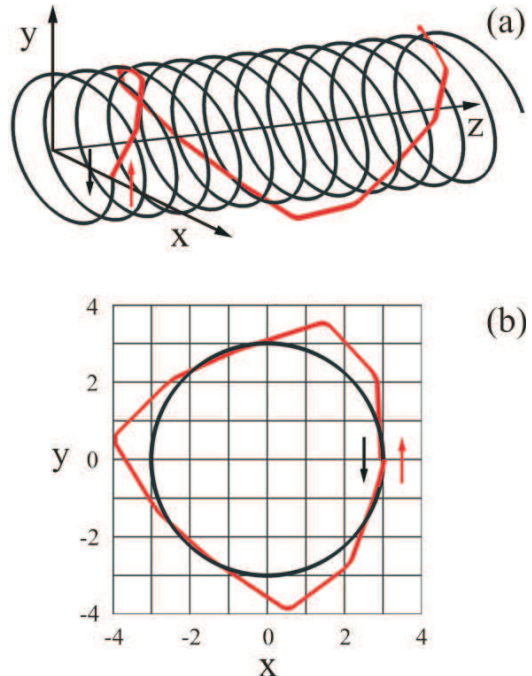


FIG. 9: Untypical trajectory of rotating soliton (red line) supported by spiral waveguide (black line): fundamental soliton is launched counterclockwise and rotates in this direction during propagation, while waveguide spirals in opposite direction. (a) 3D view for propagation distance $z = 400L_D$. (b) 2D view for $z = 294L_D$ (one period). Spiral waveguide channel has a hyper-Gaussian shape with $P_w=0.044$, $\mu = 26L_D^{-1}$ and $P=98.9$; other parameters are as in Fig. 3.

this result, we propagate a fundamental soliton in the case of small perturbations, and find that it oscillates regularly with a period in good agreement with that obtained by the Eq. (13). In such a way, main characteristics of dynamical behavior of system can be predicted from the eigenvalue procedure.

Spiraling single waveguide supports rich light beam dy-

namics. Soliton from upper power threshold, launched with a carefully chosen initial angular momentum in the direction opposite to the waveguide direction of spiraling, instead of escape from the potential barrier, becomes attracted by the spiral waveguide periodically, rapidly changing its orbit, and can be set into rotation. Such an example of untypical trajectory of rotating soliton supported by spiral waveguide is shown in Fig. 9: fundamental soliton rotates counterclockwise during propagation, while the waveguide spirals in the opposite direction.

V. VARIATIONAL APPROACH

Here, we introduce the concept and the most important ideas of the variational approach (VA) to helical waveguides and illustrate the main challenges and problems; the complete VA procedure for "slow" helical waveguid-

ing in media with arbitrary nonlinearity will be presented elsewhere.

In order to better understand dynamical phenomena concerning beam propagation along a helical waveguide, we apply a powerful approximate technique to the governing Eq. (1), based on the VA. The key idea is to decouple nonlinearity from the waveguide

$$i\frac{\partial\Psi}{\partial z} + \Delta\Psi + \Gamma I_w(x', y')\Psi + \Gamma\frac{I}{1+I}\Psi = 0, \quad (14)$$

which is justified in the shallow waveguide approximation (small I_w). After the transformation to the moving coordinate frame, in the Lagrangian density formalism we assume a Gaussian beam solution whose parameters vary along z , and make an ansatz:

$$\Psi = A \exp \left[-\frac{(x' - X_C)^2}{2W^2} - \frac{(y' - Y_C)^2}{2W^2} + iC_x(x' - X_C)^2 + iC_y(y' - Y_C)^2 + iS_x(x' - X_C) + iS_y(y' - Y_C) + i\varphi \right], \quad (15)$$

where A is the amplitude, W is the width of the beam, (X_C, Y_C) is the transverse position of the beam's center, C_x and C_y are the wave front curvatures along x and y , S_x and S_y are drift "velocity" components, and φ is the nonlinear phase shift. In the first approximation we analyze the dynamics of an axially symmetric beam in a symmetrical waveguide. In the optimization procedure, the first variation of the corresponding functional must vanish, if trial functions are chosen properly. The dynamics of the beam is described by the motion of a representative particle in the four dimensional non-stationary potential. The analysis is fairly complex, and after a lot of algebra, one obtains a nonlinear equation for beam width W

$$\frac{1}{W^2} - \frac{\Gamma I_{w0} W_w^2 W^2 (W_w^2 + W^2 - Q^2)}{(W_w^2 + W^2)^3} \times \exp \left(-\frac{Q^2}{W_w^2 + W^2} \right) - \Gamma D = 0, \quad (16)$$

where

$$Q \equiv \sqrt{X_C^2 + Y_C^2} = 2\frac{W_w^2 + W^2}{R\Omega^2 W^2} \times \left(\Gamma D - \frac{1}{W^2} + \sqrt{\left(\Gamma D - \frac{1}{W^2} \right)^2 + \frac{R^2 \Omega^4 W^4}{4(W_w^2 + W^2)}} \right), \quad (17)$$

is the transverse distance of the beam's center, and

$$D = -\frac{\ln(1 + A^2) + Li_2(-A^2)}{A^2} \quad (18)$$

is related to the beam's amplitude. The integral $Li_2(\zeta)$ defined by $Li_2(\zeta) = \int_{\zeta}^0 dt \ln(1-t)/t$ is the dilogarithm function. Equation (16) may be regarded as a procedure to find zeros numerically; for the given value of A one calculates Li_2 and D first, and after that the zeros of Eq. (16) can be found easily. In fact, there are two zeros, but only the lower one is stable.

In the dynamical case, the steady state does not exist, but one can still estimate soliton parameters. The question is, how good they are? The soliton power $P = \pi A^2 W^2$ and the width FWHM = $2\sqrt{\ln(2)} W$, as functions of the peak intensity, are shown in Fig. 10. We note good agreement between the results of variational approach and the numerical solitonic solutions for the smaller (physically more acceptable) values of peak intensity, for which the VA is valid. In this region (peak intensity between 0.1 and 7 for the given set of physical parameters, and $0.75 \leq \mu \leq 15$) where the soliton in its initial position closely overlaps the waveguide (see Fig. 7(a)), the period of small oscillations T is also calculated in a satisfactory manner (see Fig. 8). This means that the VA cannot be applied to cases of large displacement between the beam and the waveguide peak position in the equilibrium state, because Eq. (14) must be fulfilled at each transverse point.

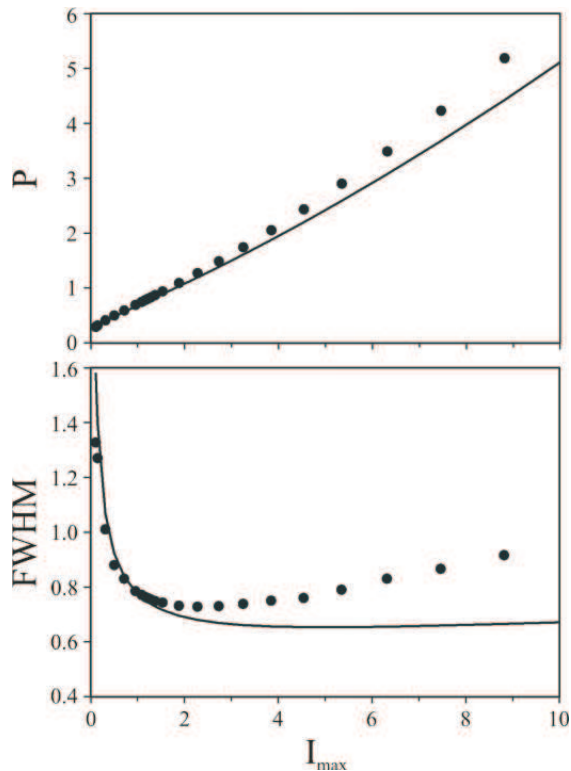


FIG. 10: Fundamental soliton power and width as functions of the peak intensity. Black dots represent stable rotary solitonic solutions obtained numerically, black solid line represents the results of the variational approach. Parameters are as in Fig. 3.

VI. CONCLUSIONS

In this paper, we have studied numerically nonlinear light propagation in a helically twisted optical waveguide formed in a photorefractive medium. We have presented a general procedure for finding exact fundamental soli-

tonic solutions in the spiraling guiding structures, based on the modified Petviashvili's iteration method. A region in the parameter space is determined, in which stable rotating solitons exist. Below the lower power threshold, the rotating solitons supported by the spiral waveguide start to radiate, and above the upper threshold they escape from the waveguide. Their stability was confirmed by direct numerical simulations. Spiralling spatial solitons supported by the 3D helical waveguide structure perform robust and stable rotational-oscillatory motion, without any signatures of radiation or decay, over many rotation periods and diffraction lengths. Inevitable numerical inaccuracy causes a regular spatial oscillation of the soliton, with the period well predicted by our calculated value.

We have developed a variational approach to find an approximate Gaussian beam solution and used it to calculate soliton parameters analytically. The "slow" helical waveguiding can be considered as a kind of dynamic localization, because the localized particle (the soliton here) periodically returns to its initial state, following the periodic change of the driving field (the helical waveguide). The spiraling single waveguide provides an excellent opportunity for studying phenomena of light propagation balanced between discreteness and nonlinearity.

Acknowledgments

This work was supported by the Ministry of Science of the Republic of Serbia under the projects OI 171033, 171006, and by the NPRP 7-665-1-125 project of the Qatar National Research Fund (a member of the Qatar Foundation). Authors acknowledge supercomputer time provided by the IT Research Computing group of Texas A&M University at Qatar. MRB acknowledges support by the Al Sraiya Holding Group.

-
- [1] Yu. S. Kivshar and G. Agrawal, *Optical Solitons: From Fibers to Photonic Crystals* (Academic, San Diego, 2003).
 - [2] L. Poladian, A. W. Snyder, and D. J. Mitchell, *Opt. Commun.* **85**, 59 (1991).
 - [3] A. Stepken, M. R. Belić, F. Kaiser, W. Królikowski, and B. Luther-Davies, *Phys. Rev. Lett.* **82**, 540 (1999).
 - [4] M. R. Belić, A. Stepken, and F. Kaiser, *Phys. Rev. Lett.* **82**, 544 (1999).
 - [5] T. Carmon, R. Uzdin, C. Pigier, Z. Musslimani, M. Segev, and A. Nepomnyashchy, *Phys. Rev. Lett.* **87**, 143901 (2001).
 - [6] O. Borovkova, V. Lobanov, Y. Kartashov, and L. Torner, *Opt. Lett.* **36**, 1936 (2011).
 - [7] M. S. Petrović, *Opt. Exp.* **14**, 9415 (2006).
 - [8] X. Wang, Z. Chen, and P. G. Kevrekidis, *Phys. Rev. Lett.* **96**, 083904 (2006).
 - [9] M. Rechtsman, J. Zeuner, Y. Plotnik, Y. Lumer, D. Podolsky, F. Dreisow, S. Nolte, M. Segev, and A. Szameit, *Nature* **496**, 196 (2013).
 - [10] Y. Lumer, Y. Plotnik, M. Rechtsman, and M. Segev, *Phys. Rev. Lett.* **111**, 243905 (2013).
 - [11] X. Zhang, F. Ye, Y. Kartashov, V. Vysloukh, and X. Chen, *Opt. Lett.* **41**, 4106 (2016).
 - [12] S. Longhi, D. Janner, M. Marano, and P. Laporta, *Phys. Rev. E* **67**, 036601 (2003).
 - [13] W. C. Henneberger, *Phys. Rev. Lett.* **21**, 838 (1968).
 - [14] S. Longhi, M. Marangoni, D. Janner, R. Ramponi, P. Laporta, E. Cianci, and V. Foglietti, *Phys. Rev. Lett.* **94**, 073002 (2005).
 - [15] S. Longhi, *Phys. Rev. A* **71**, 055402 (2005).
 - [16] I. L. Garanovich, S. Longhi, A. A. Sukhorukov, and Yu. S. Kivshar, *Phys. Rep.* **518**, 1 (2012).
 - [17] Y. Kartashov, V. Vysloukh, and L. Torner, *Opt. Lett.*

- 38**, 3414 (2013).
- [18] K. Minoshima, A. Kowalevicz, I. Hartl, E. Ippen, and J. Fujimoto, *Opt. Lett.* **26**, 1516 (2001).
- [19] M. Petrović, D. Jović, M. Belić, J. Schröder, Ph. Jander, and C. Denz, *Phys. Rev. Lett.* **95**, 053901 (2005).
- [20] M. R. Belić, D. Vujić, A. Stepken, F. Kaiser, G. F. Calvo, F. Agulló-López, and M. Carrascosa, *Phys. Rev. E* **65**, 066610 (2002).
- [21] V. I. Petviashvili, *Fiz. Plazmy* **2**, 469 (1976) [*Sov. J. Plasma Phys.* **2**, 257 (1976)].
- [22] J. Yang, I. Makasyuk, A. Bezryadina, and Z. Chen, *Stud. Appl. Math.* **113**, 389 (2004).
- [23] N. Aleksić, M. Petrović, A. Strinić, and M. Belić, *Phys. Rev. A* **85**, 033826 (2012).
- [24] N. G. Vakhitov and A. A. Kolokolov, *Radiophys. Quantum Electron.* **16**, 783 (1973).
- [25] M. R. Belić, A. Stepken, and F. Kaiser, *Phys. Rev. Lett.* **84**, 83 (2000).